Load and Sliding Velocity Effect in Dry Sliding Wear Behavior of CuZnAl Shape Memory Alloys

J. PEÑA, J.M. GUILEMANY, and F.J. GIL

The wear behavior of shape memory alloys is linked to the thermoelastic martensitic transformation. Due to this transformation, these alloys have the ability to absorb a high amount of energy before undergoing plastic deformation and subsequent fractures caused by wear. In this study, the effect of sliding velocity and load on the dry wear behavior of CuZnAl alloys has been characterized. Weight loss as a function of the M_s transformation temperature at different sliding velocities and loads was studied for the different alloys. The weight loss and friction coefficient of the alloys as a function of load showed linear and exponential relationships, respectively; however, when considered versus applied sliding velocity, independently of which phase was present, they showed an exponential relation and no direct relation, respectively.

I. INTRODUCTION

WHENEVER dry sliding occurs, mechanical energy is transformed into heat through the surface. Volumetric processes also occur in and around the real area of contact. This frictional heating, and the thermal and thermomechanical phenomena associated with it, can significantly influence the tribological behavior of the sliding components.[1,2,3]

Shape memory alloys exhibit properties that differ from those of conventional engineering materials. The shape memory effect,[4,5] superelasticity,[6,7] and damping effect[8,9] are the properties most closely linked to the martensitic transformation. This transformation can be caused by either temperature or stress. When friction occurs, temperature and stress are the two important parameters; they are more determinant parameters for shape memory alloys than in conventional materials.

Superelasticity involves the production of a martensitic transformation when an external stress is applied. The only important difference between thermal and stress-induced martensite is that the plates being formed through stress are of just one or a small number of variants, instead of being members of a self-accommodating group.[10] The variant formed is the one whose corresponding strain most relaxes the applied tensile stress in a crystal whose length is kept constant, the same variant that for a given tensile stress gives the largest tensile strain.

For copper-based shape memory alloys, the tension associated with stress-induced martensite is directly related to the transformation temperature M_s.[11,12,13] The bigger the transformation temperature M_s, the smaller the stress required to induce martensite. There is equivalence between temperature and stress in the thermoelastic process of martensite formation: a decrease in temperature is equivalent to an increase in stress, both of which stabilize the martensite phase.

Several authors[14–20] have shown that the NiTi alloy, which exhibits shape memory properties, is often more wear-resistant than conventional materials, such as some steels and Ni- and Co-based alloys. We have shown previously that CuZnAl shape memory alloys have a high dry wear resistance, β alloys proving to be more wear-resistant than the martensitic ones.[21]

II. EXPERIMENTAL PROCEDURE

Wear tests were performed using five CuZnAl shape memory alloys. The temperature range of M_s studied was from −100 °C to 50 °C. The chemical compositions and microstructures of the different alloys used are shown in Table I.

Adhesive wear tests were performed using a pin-on-disk machine according to the ASTM G99-90 standard, using 316L austenitic stainless steel disks. The dimensions of the pin were as follows: length 15 mm, diameter 3.8 mm, and curvature radius 2 mm. The experimental method and material preparation are described elsewhere.[21]

The weight loss of the pin was measured after a sliding distance of 2250 m in each test. In the wear test, five different loads (1 N, 5 N, 10 N, 15 N, and 20 N) and five different velocities (0.05 m/s, 0.075 m/s, 0.1 m/s, 0.3 m/s, and 0.5m/s) were studied. For the different load levels, a linear velocity of 0.2 m/s was applied, and for the different velocity values, a load of 6 N was applied.

III. RESULTS

A. *Wear Test Pin-on-Disk*

1. *Load and sliding velocity effect on wear behavior*

Weight loss and transformation temperatures were determined as a function of applied load and velocity. Figures 1 and 2 show the relationship between the transformation temperatures M_s and the weight loss for each alloy at each sliding velocity or load. The weight loss of the different

J. PEÑA, Assistant Professor, is with the Dept. Ciencia de Materiales e Ingeniería Metalúrgica, ETSEIB, Universidad Politécnica de Cataluña, Diagonal 647, 08028-Barcelona, Spain, and the Dept. Materiales y Diseño, Elisava Escuela Superior de Diseño, Ample 11–13, 08002 Barcelona, Spain. F.J. GIL, Professor of Materials Science, is with the Dept. Ciencia de Materiales e Ingeniería Metalúrgica, ETSEIB, Universidad Politécnica de Cataluña, Diagonal 647, 08028-Barcelona, Spain. Contact e-mail: francesc.xavier.gil@upc.edu J.M. GUILEMANY, Professor of Physical Metallurgy, Dept. Ingeniería Química y Metalurgia, Universidad de Barcelona, Martí i Franqués 1, 08028-Barcelona, Spain.

Manuscript submitted September 21, 2005.

Table I. Chemical Composition, Phase, and Transformation Temperatures for the Studied Alloys

Alloy	Pct Cu (weight)	Pct Al (weight)	Pct Zn (weight)	Phase	M_s (°C)	M_f (°C)	A_s (°C)	A_f (°C)
4	75.2	7.06	17.74	Martensite	55	29	36	60
8	76.6	7.99	15.41	β+Martensite	34	−7	21	40
14	72.3	6.66	21.04	β	−93	−106	−93	−83
21	76.4	7.81	15.79	β	5	−30	−11	14
13	77.0	8.14	14.86	Martensite	46	17	35	53

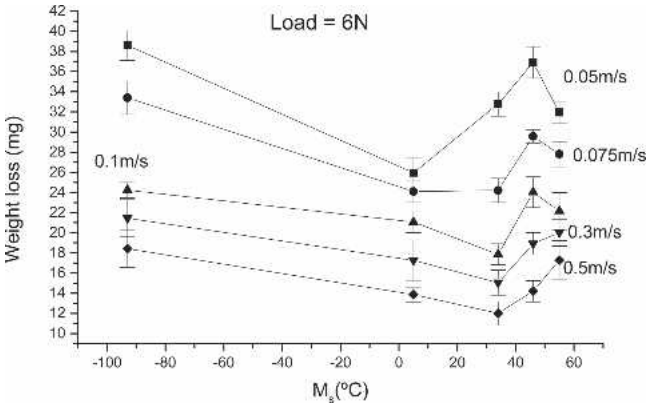

Fig. 1—Weight loss versus M_s transformation temperature for every speed parameter studied at 6 N of constant load.

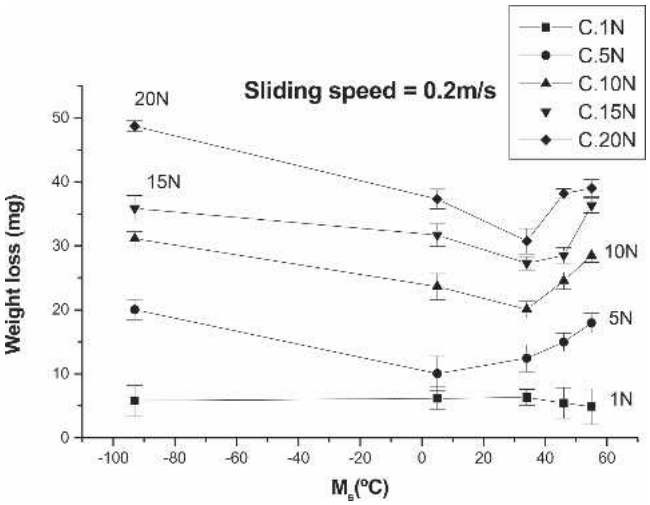

Fig. 2—Weight loss versus M_s transformation temperature for every studied load parameter at a 0.2 m/s constant speed.

alloys used in this study shows a linear dependence on load that can be fitted to Eq. [1]:

$$G = A + BN \quad [1]$$

where G = the value of weight loss (in mg) at a specific load, N = the value of the applied load (in N), A = the extrapolated value of weight loss at zero load, and B = the slope of the straight line.

The weight loss shows an exponential relationship with applied sliding velocity, independently of which phase is present, that can be fitted to Eq. [2]:

$$G = G_0 + A_1 \exp[-(v + v_0)/t_1] \quad [2]$$

Table II. Regression Values for Equation [1]

Alloy	A	B	R^2	SD
Al14	−2.82	0.46	0.9836	1.58
Al21	−1.95	0.56	0.9879	1.36
Al8	−4.22	0.74	0.9919	1.12
Al13	−3.14	0.60	0.9889	1.30
Al4	−3.04	0.52	0.9662	2.26

where G = the value of weight loss (in mg) at a specific velocity, A_1 = a constant, v = the velocity (in m/s), and t_1 = the decreased ratio of weight loss as a function of velocity. The fit of the results to Eqs. [1] and [2] is shown in Tables II and III respectively.

2. *Friction coefficients*

The friction coefficients for the different alloys studied are shown in Table IV.

The friction coefficient shows an exponential relationship with applied load that can be fitted in Eq. [3]:

$$\mu = \mu_0 + A_1 \exp[-(l + l_0)/t_1] \quad [3]$$

where μ = the value of the friction coefficient at a specific load, A_1 = a constant, l = the load (in N), and t_1 = the decreased ratio of the friction coefficient as a function of load. Eq. [3] is independent of the material phase present at room temperature. The fit of the results to Eq. [3] is shown in Table V. Contrary to previous findings for other materials, a direct relationship is not observed between the friction coefficient and sliding velocity.[2,3]

B. *X-Ray Diffraction*

After the wear tests, the stress-induced martensitic transformation of the wear surfaces was studied by X-ray diffraction (Siemens D-500, with Copper K_α radiation of λ = 1.5418 Å for 40 KV at 30 mA). The X-ray pattern of the β and martensite alloys obtained for the β-phase alloy 52 and the martensite phase alloy 24 without wear test (Standard)[21] were compared with the X-ray diffraction pattern obtained for the wear surfaces corresponding to loads of 1 N, 10 N, and 20 N, and for sliding velocities of 0.05 m/s, 0.1 m/s, and 0.5 m/s. Also, the X-ray diffraction patterns were compared with the most representative patterns obtained from the literature.[22–29] In all patterns, the angle range studied was 2θ = 35 to 100 degrees. The angle ranges between 2θ = 10 and 35 degrees did not show any representative peaks. A good correlation was seen between the X-ray patterns for alloys 52 and 24 obtained here and published patterns, with almost complete overlap of the peaks corresponding to the martensitic phase. In contrast, such an agreement was

Table III. Regression Values for Equation [2]

Alloy	$G_0 \pm \sigma$	V_0	$A_1 \pm \sigma$	$t_1 \pm \sigma$	$\chi^2 \pm \sigma$
Al14	18.96 ± 1.82	0.05	20.37 ± 2.98	0.05 ± 0.02	6.28
Al21	13.82 ± 0.44	0.05	12.23 ± 0.50	0.11 ± 0.01	0.18
Al8	12.84 ± 0.76	0.05	20.09 ± 1.09	0.04 ± 0.01	1.14
Al13	14.97 ± 0.76	0.05	22.04 ± 1.19	0.06 ± 0.01	1.02
Al4	17.91 ± 0.94	0.05	14.33 ± 1.54	0.05 ± 0.01	1.66

Table IV. Friction Coefficients for the Studied Alloys

Alloy	1 N	5 N	10 N	15 N	20 N	0.05 m/s	0.075 m/s	0.1 m/s	0.3 m/s	0.5 m/s
Al4	0.55	0.41	0.35	0.34	0.34	0.34	0.35	0.34	0.34	0.38
SD	0.08	0.05	0.04	0.03	0.03	0.03	0.02	0.01	0.04	0.02
Al13	0.53	0.48	0.50	0.11	0.31	0.35	0.38	0.42	0.35	0.39
SD	0.07	0.05	0.07	0.01	0.02	0.02	0.01	0.03	0.02	0.07
Al8	0.55	0.37	0.34	0.32	0.30	0.39	0.37	0.36	0.37	0.38
SD	0.07	0.06	0.03	0.03	0.03	0.06	0.02	0.02	0.03	0.02
Al21	0.59	0.39	0.30	0.30	0.27	0.34	0.35	0.37	0.38	0.39
SD	0.06	0.07	0.02	0.02	0.01	0.03	0.03	0.03	0.04	0.02
Al14	0.57	0.38	0.38	0.31	0.34	0.45	0.40	0.36	0.41	0.44
SD	0.06	0.04	0.02	0.02	0.02	0.08	0.02	0.03	0.03	0.03

Table V. Regression Values for Equation [3]

Alloy	$\mu_0 \pm \sigma$	N_0	$A_1 \pm \sigma$	$t_1 \pm \sigma$	$\chi^2 \pm \sigma$
Al14	0.34 ± 0.03	1	0.22 ± 0.04	3.15 ± 1.81	0
Al21	0.29 ± 0.34	1	0.29 ± 0.32	10.10 ± 26.38	0.014
Al8	0.32 ± 0.01	1	0.23 ± 0.02	2.43 ± 0.59	0
Al13	−0.09 ± 3.23	1	0.65 ± 3.16	27.37 ± 189.48	0.03
Al4	0.34 ± 0.01	1	0.22 ± 0.01	3.88 ± 0.37	0

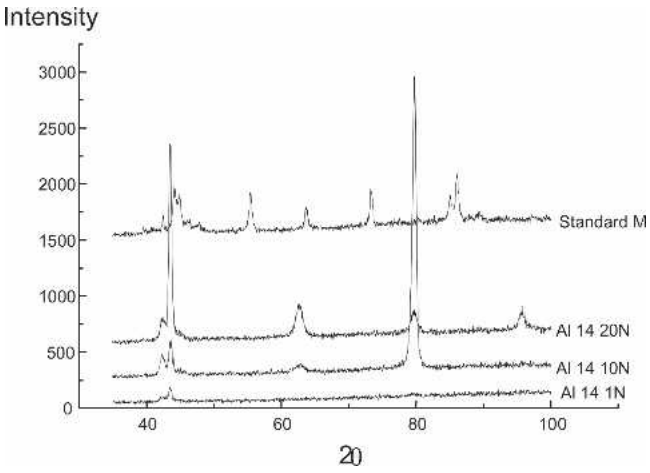

Fig. 3—X-ray diffraction patterns for alloy 14 in β phase after wear tests at different loads.

not observed for the β phase. Consequently, the group of peaks that appear between the 2θ angles of 40 and 50 degrees can be associated with the martensitic phase. At 43.60 degrees, a β-phase peak appears corresponding to the reflection of plane (220) that is impossible to differentiate from the reflections corresponding to the martensitic phase due to the high background noise.

The X-ray diffraction patterns obtained for the wear surfaces of β-phase alloys 14 and 21 are shown in Figures 3, 4, 5, and 6.

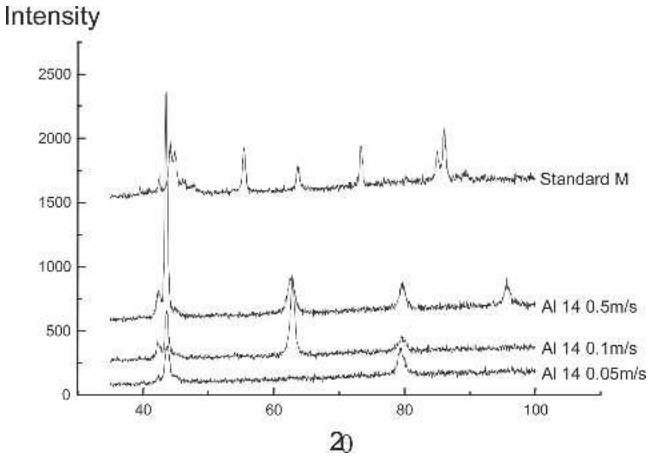

Fig. 4—X-ray diffraction patterns for alloy 14 in β phase after wear tests at different sliding speeds.

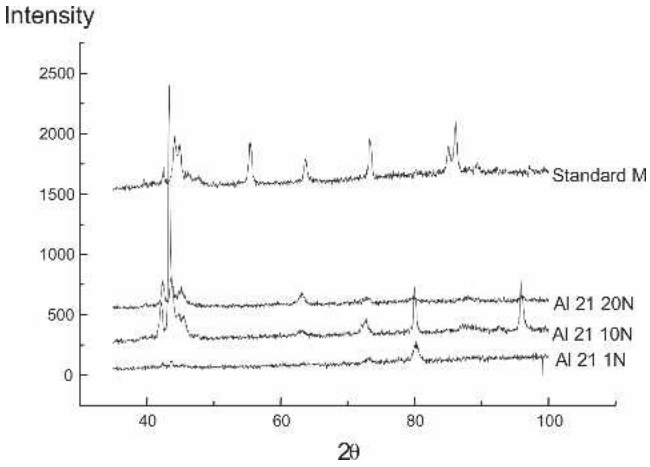

Fig. 5—X-ray diffraction patterns for alloy 21 in β phase after wear tests at different loads.

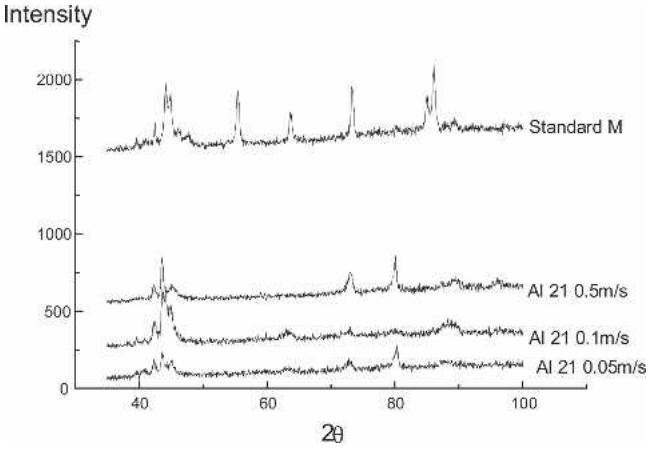

Fig. 6—X-ray diffraction patterns for alloy 21 in β phase after wear tests at different sliding speeds.

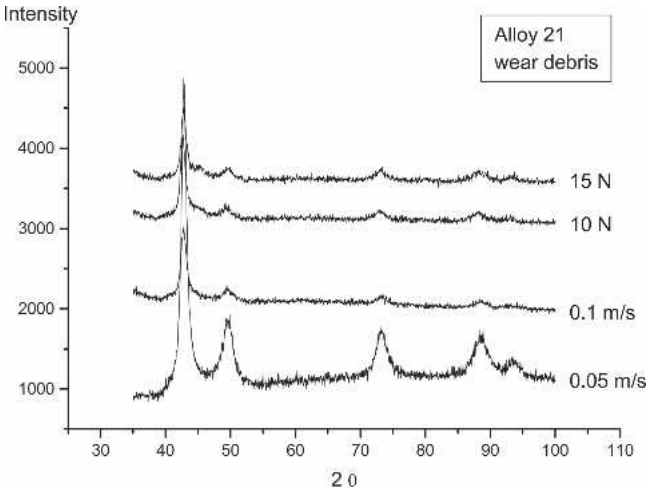

Fig. 7—X-ray diffraction patterns for the wear debris of alloy 21 in β phase after wear tests at different loads and sliding speeds.

In the cases of β-phase alloys 14 and 21, the results show that the β- and martensitic phases coexist in the wear surfaces. In both alloys, when the load or velocity is increased, the number of martensitic peaks increases. This observation would be justified in the load case by the amount of stress-stabilized martensite (SIM). The larger the load, the more SIM presents in the wear surfaces.

For the β+ martensite alloy 8, as in the previous case, coexistence of the β and martensitic phases was observed.[26] For the martensitic alloys, only martensitic peaks appeared. The wear process causes a reorientation of the martensitic plates, as indicated by the fact that, in addition to the peaks present in the X-ray pattern of alloy 24 without wear test, other peaks also appear; some of these additional peaks have been described previously,[22–25] while others are yet to be identified. Similarly, some peaks that appear in the X-ray pattern of the wear surfaces do not appear in that of the unworn surfaces.[26]

X-ray patterns for the wear debris of the different alloys studied were also obtained. Figure 7 shows four representative X-ray patterns for the wear debris of the β-phase alloy 21. All X-ray patterns for the wear debris were similar, independently of the phase and the parameter studied. Only the martensitic phase was found to be present in the wear debris.

IV. DISCUSSION

A. *Load and Sliding Velocity*

The results presented in Figures 1 and 2 are in agreement with those described previously.[21,26] In these studies, the wear behavior for the CuZnAl alloy is related as a function of the M_s transformation temperature. Independently of velocity, and for loads higher than 1 N, we observed that the room temperature β alloys (14 and 21) exhibit a wear behavior marked by the ease of producing stress-induced martensite. The transformation was more easily produced in alloy 21, implying greater wear resistance. The depth of the stress-induced martensitic transformation mainly depends on the M_s. For alloy 21 in β phase, it is about 120 μm when 10 N is applied. The depth of the stress-induced martensite is similar for larger loads applied, only changing the amount and size of the martensitic plates. After wear test, the stabilized stress-induced martensite is not observed for alloy 14.

For the martensitic and β+ martensitic alloys, the results do not exhibit a direct relationship: they are independent of Ms transformation temperature and applied load and applied velocity. For the high values of velocity and medium loads studied, the wear behavior exhibited by the material is as predicted. The greater the ease of producing reorientation and coalescence of the martensitic plates, the greater the wear resistance exhibited by the alloy.

Different velocities change the amount of sliding, the number of impacts, and the number of revolutions that occur within a unit of time. These changes cause a pseudochange in wear behavior, namely a change in wear rate per unit time. Beyond this, the effect of velocity is generally negligible, except when one or more of the following conditions occur:[27]

(1) Temperature increases sufficiently to affect material properties.
(2) Temperature increases to affect or introduce chemical wear processes.
(3) Formation and stability of tribofilms are affected.
(4) Mechanical response of a viscoelastic material is affected.
(5) Thickness or formations of hydrodynamic films are affected.
(6) There is a lubrication breakdown.

For this study, the two first conditions play an important role and the other conditions are irrelevant. For the effects of load and sliding velocity on wear resistance, two equations have been fitted that relate these two parameters to the material weight loss. First, the sliding velocity versus weight loss for a constant load relationship follows an exponential equation (Eq. [2]). The effects of sliding on wear behavior are generally caused by changes in frictional heating, oxide formation, and tribofilm formation.[27]

In shape memory alloys, an increment in surface temperature caused by different sliding velocities or loads affects the material properties, so it is very important to consider the increased temperature arising from frictional heating that is implicit in the sliding velocity term. When increasing the

sliding velocity, the disk and pin surface temperatures increase, causing a more ductile material behavior than seen at lower temperatures. This temperature plasticity effect causes a decrease in the material weight loss. Also, stress-induced martensitic transformation and the reorientation and coalescence of martensitic plates should be considered, as they represent the most significant adaptation for either surface and an important mechanism associated with shape memory alloys. Similarly, transformation stress induces martensite to form the β phase, occurring through the effect of skin temperature (frictional heating), causing a high energy loss and a consequent hardening of the material.[21,26] All these coordinated factors lead to the improvement of the dry sliding wear behavior when the sliding velocity increases. In this way, the precise temperature of the surface pin in relation to the sliding velocity and load applied has been estimated by the Lin and Asbhy equation,[3] showing in both that the increase is very small. However, the equation does not take in account the energy associated with the thermoelastic transformation. For high sliding velocities (0.2 to 0.5 m/s), the wear can be described as mild, as indicated in Eq. [2]. However, for low sliding velocities, taking into account the wear surfaces, wear also can be described as mild (Figure 8).

A parallel analysis of the relationship between load and weight loss shows a linear relationship of the type described by Eq. [1]. In this case, an exponential relationship between the friction coefficient and the applied load is also observed, similar to the one observed between sliding velocity and weight loss. The largest friction coefficient was obtained for a 1 N load, but also the smallest weight loss. This observation may be due to two factors. The first is that for this load, material hardness provides the principal explanation for the wear behavior (theory of tribology). There is no stress-induced martensitic transformation or martensitic reorientation, so the shape memory properties do not play a significant role in the wear behavior at this load. For all the studied alloys, the results of the metallography and XRD analysis have shown that no stress-induced martensite and no reorientation of martensite plates are produced after the wear test at 1 N of applied load.[21] The second is that a 1 N load is insufficient to easily remove the wear debris that forms toward the exterior of the sample, thereby generating an oscillation in the normal force that is applied in the wear process.

For these applied loads (1–20 N), the wear can be described as mild, as indicated by Eq. [1] for all materials studied. The wear surface for alloy 21 at 20 N (the most severe wear for the loads studied) is shown in Figure 9.

B. *Wear Model*

A theoretical justification of these effects is obtained starting from the adhesion theory. According to this theory,[1] the effective surface area for elastic contact A_r is proportional to the normal force $F_N^{2/3}$.

In this way:

$$A_r \alpha F_N^{2/3} = P_0^{2/3}/A^{2/3} \quad [4]$$

where P_0 = the material contact plastic transition pressure and A = the apparent contact area.

Using this as a starting point, $A_r \alpha P_0^{2/3}$, and the friction coefficient is:

$$\mu = F_T/F_N = \tau(A_r)/P_0(A) \quad [5]$$

where F_T = the friction force and τ = the shear stress. This equation is based on the assumption that there is no structure and no chemical composition changes. In shape memory alloys there is a structural change when load and temperature affected the material.

From this, we can conclude that, in the elastic contact case, a friction coefficient decrease is defined as a function of the applied load, as can be seen in Table V.

In general, it is assumed that the real contact area in the wear process consists of a high degree of microroughness, or microprotuberances, more or less in uniform contact inside the nominal contact area. However, this suggestion is not always certain, especially when the sliding velocity is high (due to surface accommodation processes).

Despite this, one can affirm that, independently of the geometry of the real contact area, the energy dissipation during friction and the origin of the friction force take place within this real contact area.

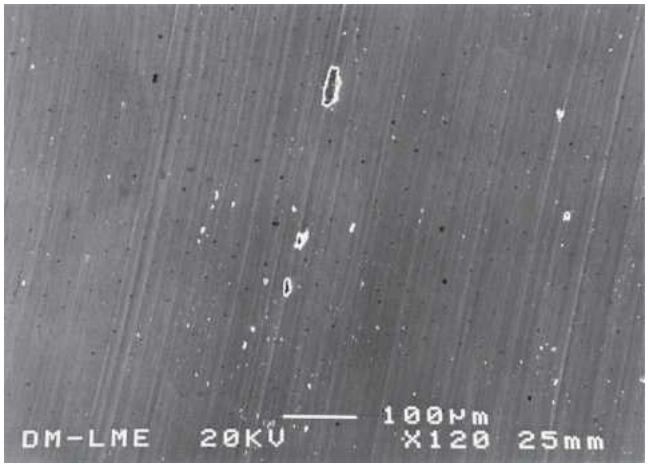

Fig. 8—Wear surface for alloy 21 at 6 N load and 0.05 m/s sliding speed, in which severe wear is not observed.

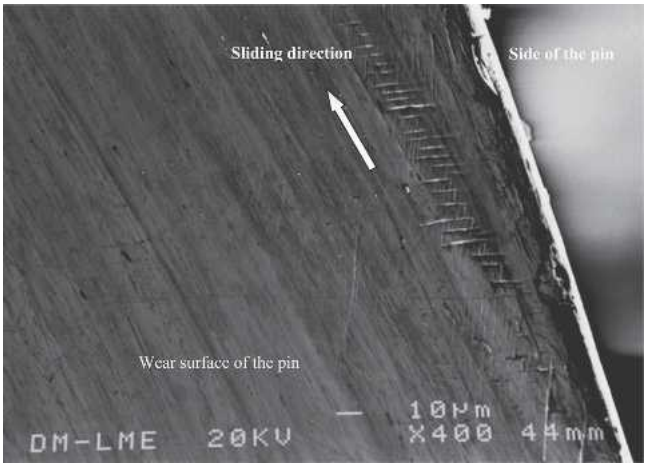

Fig. 9—Wear surface for alloy 21 at 20 N load and 0.2 m/s sliding speed, in which severe wear is not observed.

The fundamental premise on which tribology is based is the existence of a different sliding velocity between the elements that are in relative motion. Berthier *et al.*[28,29] present a model that accommodates the different sliding velocity between the bodies in relative movement, concluding that each body (five bodies) can participate in the deformation accommodation, in four different ways, called accommodation ways. These are as follows:

(1) Elastic deformation
(2) Rupture
(3) Nonreversible shear
(4) Roller formation

The five bodies and four deformation modes combined define 20 possible accommodation mechanisms in a contact. The prevalence of one or another depends on the test conditions.

In this way, one can think that the friction that is believed to take place when slip occurs between two bodies has two basic sources: (*a*) the interfacial bond in the contact interface and (*b*) the material deformation in and around the contact areas. The first contribution has a strong influence on the friction force. This influence depends on surface cleaning and sliding material compatibility; it is a skin effect. It also contributes directly to the frictional energy through the irreversibility associated with the breaking and formation of adhesive bonds in the real contact area. The contribution of deformation is a volumetric effect and includes two types of plastic deformation: the first type due to scratches or riles caused by the harder surface on the soft surface, and the second due to plastic deformation near the surface that takes place as a consequence of the traction of the areas where adhesion occurs. Both contributions affect frictional energy through the work done by the plastic deformation of the two materials that slip (in all systems in which dry slip takes place, there are sources of superficial friction and volumetric friction).

Based on these premises, a comparative study can be performed to assess the importance of each. Protasov *et al.*[30] carried out a study of both effects and concluded that the amount of dissipated energy in the near surface layers can significantly exceed the energy dissipated at the contact surface. This is particularly valid for metals with high thermal conductivity. They estimate that for copper sliding on steel, more than 85 pct of the frictional energy is dissipated by a volumetric process based on plastic deformation. Prior to this, Rigney *et al.*[31,32] developed a model for friction based on energy. In this model, they assume that the frictional energy dissipates through plastic deformation in the layers near the surface, and they reject the direct process adhesion contribution because it is too small. This deformation will be qualitatively indicative for the energy absorption process that takes place in the material.

Figures 10 and 11 how this volumetric deformation phenomenon occurring in the slip direction. The different shadings of the martensitic plates are different martensite variants favored by the sliding direction. In this way, the results obtained are in agreement with those outlined by Protasov *et al.*,[30] considering that for the copper-based shape memory alloys used in this study, a high quantity of frictional energy is dissipated by a volumetric process consistent with plastic deformation.

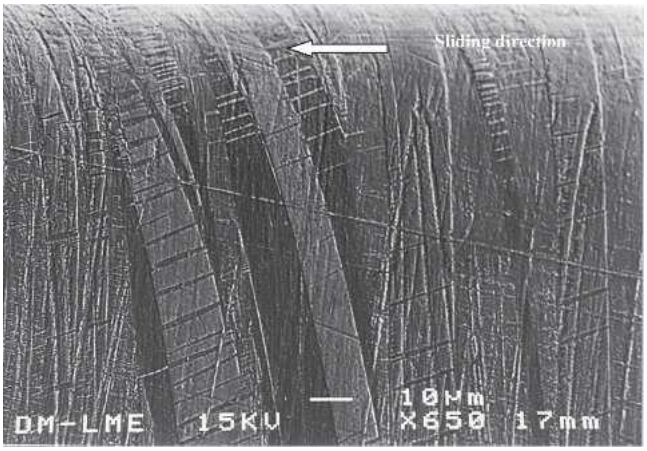

Fig. 10—Plastic deformation in the wear surfaces for alloy 4 in martensitic phase after wear tests at a load of 20 N and a sliding speed of 0.2 m/s.

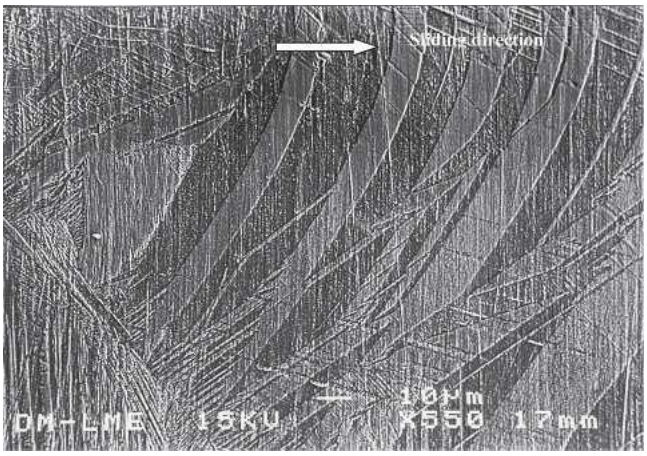

Fig. 11—Plastic deformation in the wear surfaces for alloy 13 in martensitic phase after wear tests at a load of 20 N and a sliding speed of 0.2 m/s.

The plastic deformation process of shape memory alloys is different from the process that occurs in conventional materials, the amount of absorbed energy being much larger in these alloys.

The fact that the deformation process will be different for different alloy compositions is worth highlighting. β-phase alloys will be deformed according to a superelastic behavior, while the martensitic phase will be deformed by means of the reorientation, coalescence, and twinning of martensitic plates, also by plasticity. The frictional energy absorption process will therefore be larger, or more effective, in the β-phase alloys with an easy transformation (high M_s) and $\beta+$ martensite than in the martensitic phase. This difference in the absorption process means that for the different sliding velocities, the effect that the temperature has on the material will vary according to the phase that is present at the test temperature (M_s). This is the cause of the irregular behavior of the friction coefficient representation versus the sliding velocity obtained in this work.

Similarly, the X-ray results for wear debris in all the alloys studied, regardless of the M_s transformation temperature (Table I), show that they are in the martensitic phase. This

martensitic phase is stable at the test temperature: "thermomechanically stabilized martensite."

V. CONCLUSION

The weight loss and friction coefficient of the different alloys used in this study, as functions of load, show a linear relationship and an exponential relationship, respectively. The weight loss and friction coefficient versus applied sliding velocity, independently of which phase was present, show an exponential relationship and no direct relation, respectively.

The dissipated energy in the layers near the surface is responsible for the good dry sliding wear behavior of the CuZnAl shape memory alloy. The critical stress for inducing martensite and the energy absorption capacity before plastic deformation and subsequent fractures are the important parameters to explain the wear resistance. The wear resistance that a material exhibits is a property that is affected by highly diverse parameters that are sometimes difficult to control. For this reason, the results obtained sometimes display large dispersions. The inclusion of a higher number of test samples in future studies may help to reduce this effect.

REFERENCES

1. G. Zambelli and L. Vicent: *Matériaux et Contacts*, Presses Polytechniques et Universitaires Romandes, Lausanne, 1998.
2. E. Rabinowicz: *Friction and Wear of Materials*, John Wiley & Sons Inc., New York, 1995, pp. 245-59.
3. S.C. Lim and M.F. Ashby: *Acta Metall.*, 1987, vol. 35, pp. 105-07.
4. L.C. Chang and T.A. Read: *Trans. AIME.*, 1951, vol. 191, pp. 47-48.
5. W.J. Buehler, J.W. Gilfrich, and R.C. Willey: *J. Appl. Phys.*, 1963, vol. 34, pp. 1475-80.
6. J.M. Guilemany and F.J. Gil: *Rev. Metal. Madrid*, 1990, vol. 26, pp. 164-70.
7. H. Horikawa, S. Ichinose, K. Morii, S. Miyazaki, and K. Otsuka: *Metall. Trans. A*, 1988, vol. 19A, pp. 915-19.
8. H.C. Lin, S.K. Wu, and Y.C. Chang: *Metall. Mater. Trans. A*, 1995, vol. 26, pp. 851-54.
9. Y. Liu and J. Van Humbeeck: *Journal de Phys. IV. Coll. C 5 Supl. au Journal de Phys III*. 1997, vol. 11, pp. 519-20.
10. H.C. Tong and C.M. Wayman: *Acta Metall.*, 1974, vol. 22, pp. 887-90.
11. H. Funakubo: *Shape Memory Alloys (Vol. 1)*, Plenum Press, New York, 1987.
12. K. Otsuka, C.M. Wayman, K. Nakai, H. Sakamoto, and K. Shimuzu: *Acta Metall.*, 1976, vol. 24, pp. 207-11.
13. W. Arneodo and M. Ahlers: *Acta Metall.*, 1974, vol. 22, pp. 1475-80.
14. D.Y. Li: *Scripta Mater.*, 1996, vol. 34, pp. 195-201.
15. J. Jialing and W. Hongliang: *Acta Metall. Sinica Ser. A*, 1988, vol. 1, pp. 76-89.
16. R.H. Richman, A.S. Rao, and D. Kung: *Wear*, 1995, vol. 181, pp. 80-86.
17. Y.N. Liang, S.Z. Li, Y.B. Jin, W. Jin, and S. Li: *Wear*, 1996, vol. 198, pp. 236-50.
18. Y. Shida and Y. Sugimoto: *Wear*, 1991, vol. 146, pp. 219-25.
19. R.H. Richman, A.S. Rao, and D.E. Hodgson: *Wear*, 1992, vol. 157, pp. 401-10.
20. R. Liu and D.Y. Li: *Metall. Mater. Trans. Vol. A*, 2000, vol. 31A, pp. 2773-77.
21. J. Peña, F.J. Gil, and J.M. Guilemany: *Acta Mater.*, 2002, vol. 20, pp. 3115-19.
22. J. Gui, C. Luo, H. Zhang, W. Hu, and R. Wang: *J. Mater. Sci.*, 1990, vol. 25, pp. 1675-80.
23. T. Suzuki, R. Kojima, Y. Fujii, and A. Nagasawa: *Acta Metall.*, 1989, vol. 37, pp. 163-70.
24. D. Shi, J. Gui, S.S. Tan, and R. Wang: *Mater. Sci. Eng., B*, 1998, vol. 56, pp. 31-50.
25. Z. Yubin and W. Weimin: *ICOMAT*, 1994, vol. 94, pp. 389-91.
26. J. Peña: Doctoral Thesis, Universidad Politécnica de Cataluña, Barcelona, 2000.
27. R.G. Bayer: *Wear Analysis for Engineers*, MNB Publishing, New York, 2002.
28. "Mécanismes et tribologie", *Thèses Science*, INSA Lyon, no. 88 INSAL 0050, 1988.
29. Y. Berthier, L. Vincent, and M. Godet: *Eur. J. Mech. A/Solids*, 1992, vol. 11, pp. 35-40.
30. B.V. Protasov and I.V. Kragelskii: *Sov. J. Wear*, 1982, vol. 2, pp. 101-08.
31. D.A. Rigney and J.P. Hirth: *Wear*, 1979, vol. 53, pp. 345-55.
32. P. Heilmann and D.A. Rigney: *Wear*, 1981, vol. 72, pp. 195-204.